Draft version April 11, 2023
Typeset using LaTeX **twocolumn** style in AASTeX631

Physics 111B Lab Report: Atomic Physics

Yubin Hu[1]

[1]*Department of Physics, University of California, Berkeley, CA 94720-3411, USA*

ABSTRACT

In this lab, we perform spectroscopy and interferometry on Hydrogen and Helium to measure two important constants in atomic physics: the Rydberg constant and the Bohr magneton. Our measurements confirmed the first three significant digits of the Rydberg constant while the underestimation in our errors may have resulted in a disagreement in the fourth significant digit. For the Bohr magneton, we measured a value significantly higher than the accepted value, which is likely due to systematic underestimation in our experiment of the magnetic field strength used for Zeeman splitting.

Keywords: Atomic Physics, Zeeman Effect, Monochrometer, Fabry–Pérot

1. INTRODUCTION AND THEORY

1.1. *Hydrogen Spectrum and the Rydberg Constant*

A hundred years after the invention of quantum mechanics, the fact remains that, for most atoms, theoretical prediction of their energy levels using quantum mechanics is hard if not impossible (Holzapfel (2023)). With only a single electron orbiting the nucleus, Hydrogen is an amazing exception. With some simplifications, the nth energy level of Hydrogen can be expressed as

$$E_n = -\frac{hcR}{n^2} \tag{1}$$

where R is the Rydberg constant.

When the electron falls from a $n > 2$ level to the $n = 2$ level, it emits a photon in the visible light range. The energy carried by this photon equals the energy difference between the two levels, and its wavelength λ_n can be calculated as the following:

$$\frac{1}{\lambda_n} = R(\frac{1}{4} - \frac{1}{n^2}) \tag{2}$$

By measuring the wavelength of these photons through spectroscopy, therefore, we can approximate the Rydberg constant.

1.2. *Helium Spectrum*

The helium spectrum is more complicated and all we need to know for this experiment is that are singlets and triplets states where total electron spin $S = 0$ and triplet states where the total electron spin $S = 1$. They correspond to different Zeeman splittings. The triplet state splittings are significantly more complicated and cannot be measured with our current instruments, so we focus on the Zeeman effect for the singlet states in this experiment.

1.3. *Normal and Anomalous Zeeman Effect*

Similar to the current loop generating a magnetic dipole perpendicular to the loop, electrons orbiting the nucleus in atoms generate a magnetic dipole moment parallel to the electron orbital angular momentum.

When we put the atom in an external magnetic field, this magnetic dipole moment interacts with the magnetic field. The total energy of the atom change based on how aligned its magnetic dipole moment is with the magnetic field. This change in energy levels is observable and therefore is a measurement of the orbital angular momentum along the magnetic field direction. This measurement forces the observable "orbital angular momentum along the magnetic field direction" to collapse into discrete states each signified with the magnetic quantum number $m_J \in \{-J, -J+1, ..., J\}$, where J is the total orbital angular momentum quantum number.

In the regime where the magnetic field is weak, the electrons in energy levels with orbital angular momentum quantum number m_J get shifted to a new energy level

$$E_{m_J} = E + g_J m_J \mu_B B \tag{3}$$

where g_J is the Lande-g factor and $\mu_B = \frac{e\hbar}{2m_e}$ is the Bohr magneton.

The energy of a photon emitted due to a transition is

$$\Delta E = (E' - E) + (m'_J g'_J - m_J g_J) B \mu_B \tag{4}$$

where B is the magnetic field, and $\mu_B = \frac{e\hbar}{2m_e}$ is the Bohr Magneton. The emitted photon has quantized angular

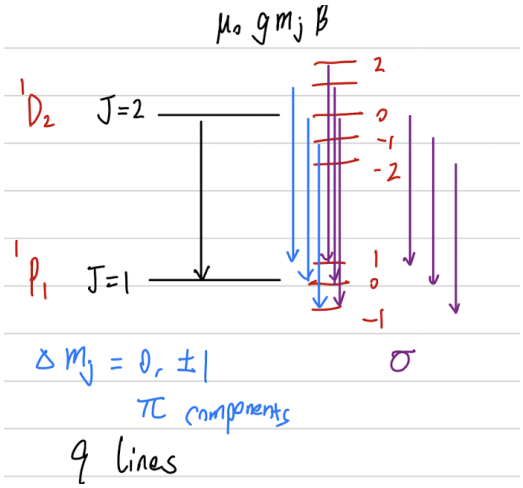

Figure 1. Zeeman Splitting for a parahelium transition

momentum, so $\Delta m_J = m'_J - m_J = \{-1, 0, 1\}$. g_J is the Lande g-factor, a proportionality constant given by

$$g_J = 1 + \frac{J(J+1) + S(S+1) - L(L+1)}{2J(J+1)} \tag{5}$$

Due to historical reasons, we distinguish between the normal Zeeman Effect that occurs when $g_J = g'_J$ and the anomalous Zeeman effect. For singlet states of helium where $S = 0$, $g_J = 1$. In the normal Zeeman Effect, a degenerate transition between two energy states splits into three transitions. π transitions occur when $\Delta m_J = 0$, and σ transitions occur when $\Delta m_J = \pm 1$

Figure 1 Shows the π (blue) and σ (purple) components of a singlet transition with Zeeman splitting. As we can see, the π component remains the same as the original transition without a magnetic field, while two σ components appear at energies $g_J m_J \mu_B B$ above and below the original transition.

1.4. *Fabry-Perot Interferometer*

The splittings caused by the Zeeman effect correspond to a wavelength difference too small to be detected by our spectrometer. To measure the energy difference between the π and σ components under Zeeman splitting, we utilize a Fabry-Perot Interferometer. A Fabry-Perot interferometer is basically two somewhat transparent mirrors placed exactly parallel to each other at a small distance.

As seen in Figure 2, incident light of wavelength λ comes at a small angle θ, and depending on these two parameters the out-going light either constructively or destructively interferes, with the maximum brightness achieved when the following equation satisfies:

$$m\lambda = 2t\cos\theta \tag{6}$$

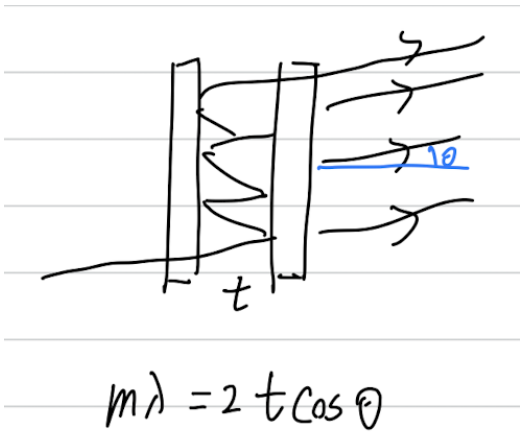

Figure 2. Fabry-Perot Illustration

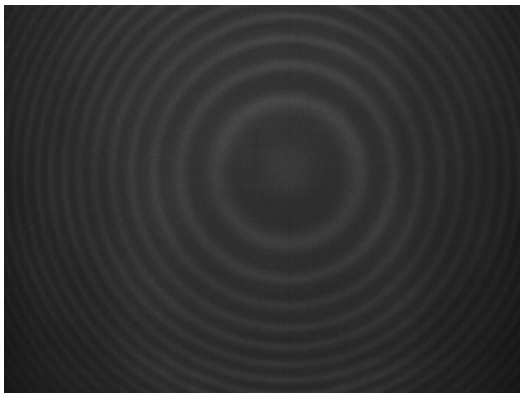

Figure 3. Fabry-Perot Interference Pattern

where m is an integer number.

When imaged with a camera, these interference patterns become a series of rings as seen in Figure 3. If the incident light wavelength changes slightly, the radius of these rings changes in a predictable manner. Thus when a magnetic field is applied to the atoms and the Zeeman splitting happens, we observe that one ring splits into multiple, and by a smart measurement of the relative radii of the rings and comparing them to the original ring radii, we can calculate the splitting size.

If we label the rings as in Figure 4, then the final equation used to calculate the Bohr magneton is

$$\mu_B = \frac{hcC_0}{4Bt}(R_{k_+}^2 - R_{k_-}^2) \tag{7}$$

where

$$C_0 = \frac{k}{R_k^2 - R_0^2} \tag{8}$$

(Hunt (2018)).

Since all length scales cancel out for the calculation for Bohr magneton, we can measure the radii in any unit. We use the number of pixels.

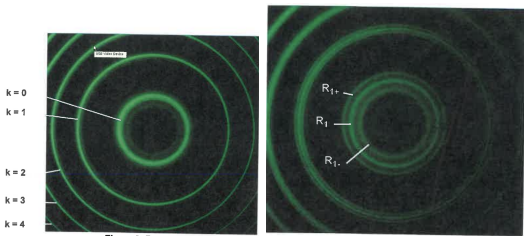

Figure 4. Zeeman Illustration

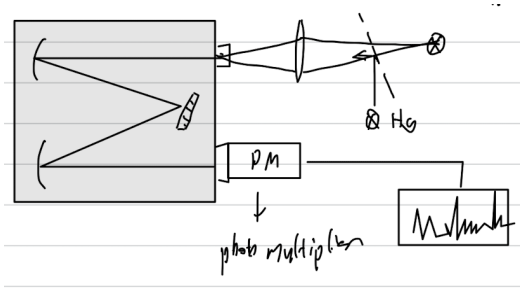

Figure 5. Rydberg Constant Apparatus

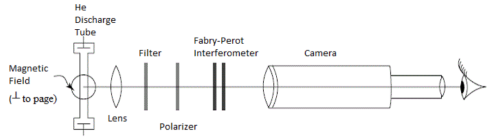

Figure 6. Bohr Magneton Apparatus

2. APPARATUS AND PROCEDURE

For the Rydberg constant experiment, the apparatus is shown in Figure 5. Light from an atomic lamp is focused by a converging lens onto the input slit of an ARC model AM-505 scanning monochromator. The monochromator contains two reflective mirrors ensuring that the light is collimated when it hits the differential grating in the middle. The grating reflects light of different wavelengths at different angles and therefore we are able to selectively measure the light intensity of a specific wavelength with the photomultiplier. As the program scans the angle of the grating, we get a spectroscopy of a range of wavelengths.

For the Bohr magneton experiment, we place the Helium lamp in a magnetic field generated by two magnetic coils in a Helmholtz configuration. Lights emitted from the lamp are focused and passed through a Fabry-Perot interferometer and imaged with a camera. This entire setup is illustrated in Figure 6.

3. DATA COLLECTION

For the Rydberg constant experiment, data on the wavelength and intensity are collected by a computer with a lab view program. We first use a Mercury lamp with known wavelengths to calibrate the spectrometer and then take measurements of the Hydrogen atom.

For the Zeeman experiment, radius data is measured from images taken with a digital camera, and the magnetic field data is measured by moving out the Helium lamp and inserting a magnetometer. The magnetic field is especially challenging since the magnetometer needs to be placed exactly at the center of the coils and faced in the correct direction. In practice, we recorded the output of the magnetometer as we move the measurement tip in the coil slowly and picked the largest number recorded as the final measurement.

4. ANALYSIS

4.1. *Rydberg Constant*

We first calibrated the spectrometer. We took measurements of a Mercury lamp in a range of about 400nm to 700nm and identified the six most prominent peaks. We selected a window around these peaks and fitted a Gaussian peak to obtain the peak wavelength and uncertainty (Figure 7). The Gaussian peak we used follows the form

$$y = A\exp(\frac{-(x-\mu)^2}{2\sigma^2}) + 0.11 \tag{9}$$

where y is the intensity and x is the wavelength. We do not leave the baseline as a variable because this reduces the degrees of freedom of our model and we do not want the optimization algorithm to fit the baseline. A constant of 0.11 is added to account for the baseline intensity. As we can see in Figure 7 the fits are good and well-centered, justifying our model design choice.

We then matched these peaks to the accepted values from the National Institute of Standards and Technology (Kramida et al. (2022)). A linear model is then used to compare the measured values and accepted values. All later measurements are transformed with this linear model. The fit and residual plots can be found in Figure 8. The fitted slope and y-intercept for calibration are 1.00100 ± -0.00011 and 8.81 ± -0.06 nm respectively. The reduced χ^2 calculated for this calibration fit is 121.84301.

After calibration, we took the spectrum data of Hydrogen and found the peaks corresponding to the Balmer Series by fitting the same Gaussian to the peaks. This Gaussian peak fit can be found in Figure 9. As we see the Gaussians are well-centered to the data peaks. Something to notice is that for the lower wavelengths, the intensity of the peak is relatively low. In fact, some noise peaks have higher prominence than the $n = 7$ and $n = 8$ transition peaks. Despite the weakness of these signals, six Balmer peaks are visible as seen in 9.

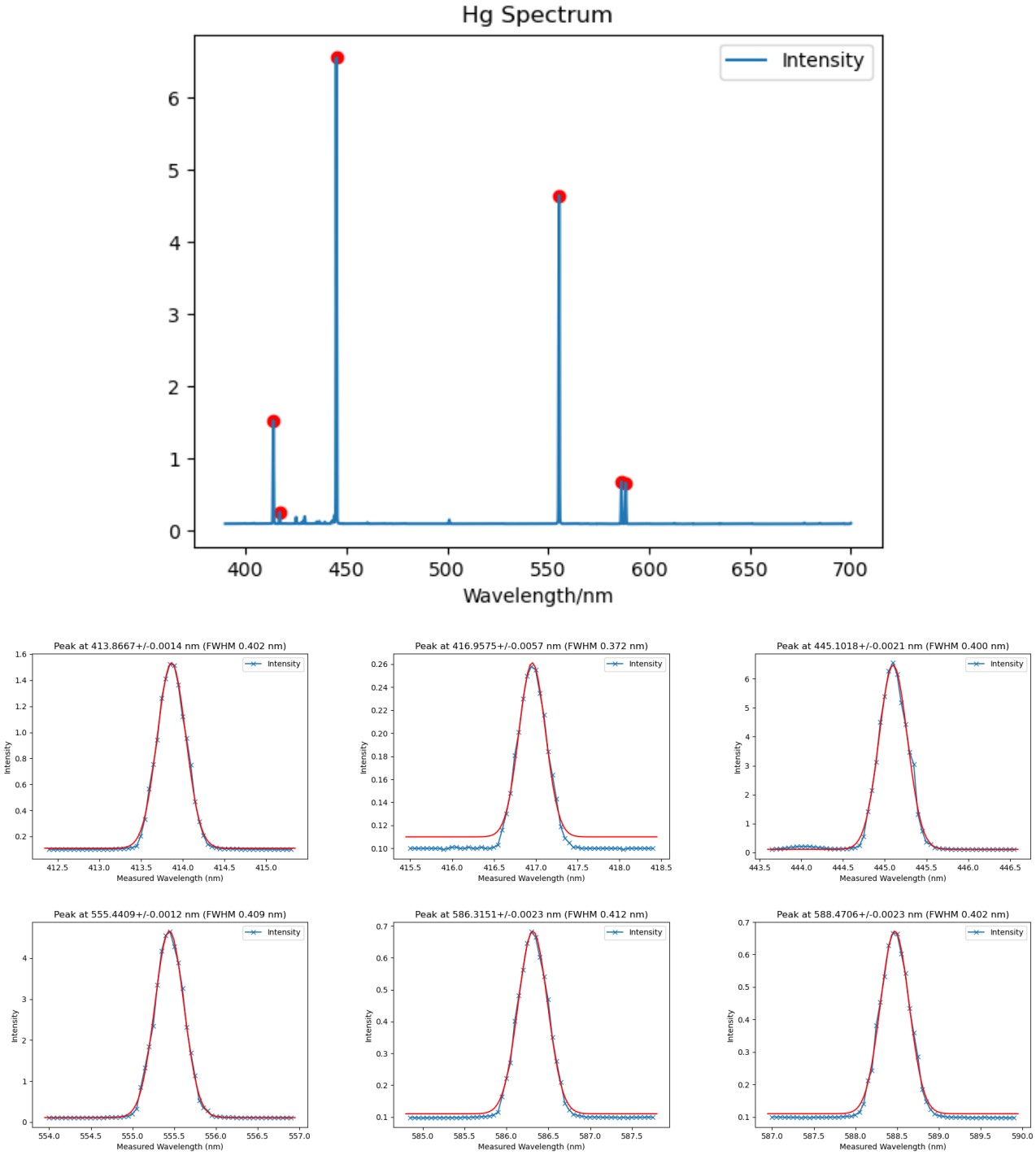

Figure 7. Hg Calibration Data

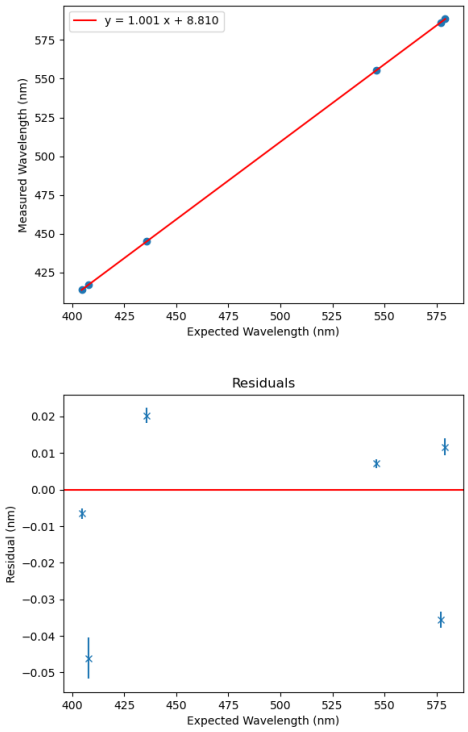

Figure 8. Calibration Fit

The small signal results in higher uncertainties in the final peak location measurements. Note also that in the figures the x-axis denotes the measured (uncalibrated) wavelength. After identifying the peak locations with uncertainties, we then apply the linear transform found via measuring the Mercury spectrum and find out the calibrated measured wavelengths.

After obtaining the calibrated Balmer series wavelengths with their uncertainties, we calculate the values $1/\lambda_n$ and $1/n^2$ and plot them (Figure 10). Then according to equation 2, the Rydberg constant is just the slope of the linear fit. We obtained the value of the Rydberg constant to be (1.0983+/-0.0005)e+07 1/m. The accepted value is 1.0973731568508e7 1/m. Our measurement agrees with the accepted value to 3 significant digits.

4.2. *Bohr Magneton*

For the Bohr Magneton experiment, there are two kinds of data we measured. The first is the radius of the relevant rings, and the second is the magnetic field strength.

We measure the radius of the rings by manually identifying five points that lie on the circle, then calculate the circle center location and radius via least squares. Uncertainties are estimated by utilizing the redundancy in our data (you only need three points to fix a circle) and calculating the standard deviations of the radius estimated using different combinations of the points.

After estimating the radii of the rings, we plug into equation 8 to obtain the value of C_0, and then into equation 7 to calculate the Bohr magneton. We report a value for Bohr magneton to be $mu_B = 1.20 \pm 0.1210^{-23} \frac{J}{T}$. This value is slightly larger than the accepted value. We will discuss this in detail in the Discussion section.

5. DISCUSSION AND CONCLUSION

We present analysis and measurement results of two fundamental atomic physics constants: the Rydberg constant and the Bohr magneton, by measuring transitions in Hydrogen atoms and Helium atoms in a magnetic field.

Our measurements for the Rydberg constant somewhat agree with the accepted value (Figure 11). The values agree to the level of one one-thousands, but the variance is higher than one standard deviation. We have underestimated the uncertainty levels. This is likely because of the calibration step. The reduced ^{2} of the calibration linear fit is 121.84301, which is significantly larger than 1, meaning that either the uncertainty on Mercury peaks is underestimated or that a linear model is not sufficient in calibrating the instrument. Since the Gaussian fits utilized many data points and the fits are visually good, we lean towards the second explanation. It is likely that the systematic errors in the spectrometer cannot be well described by a linear model. Doing a more careful analysis of the errors on the spectrometer and using a more complex model will help us reach a more accurate measurement of the Rydberg constant. This requires calibrating with potentially many atoms so that reference peaks are dense and we can have a more detailed characterization of the systematic errors. For now, since we do not have this more complex model and are approximating with a linear calibration model, we introduce uncertainties not accounted for by the uncertainties in model parameters. Therefore, our final measurement for the Balmer series does not account for the error model uncertainty either.

Our measurements for the Bohr magneton are significantly higher than the accepted value. This is likely because of a systematic underestimation of the Zeeman magnetic field. Since the Helium lamp is located exactly at the center of the magnetic coils where the magnetic field is the strongest, and the magnetometer may not be exactly at the center and may not face exactly in the direction of the magnetic field (both reduces the measured strength of the magnetic field), the magnetic field

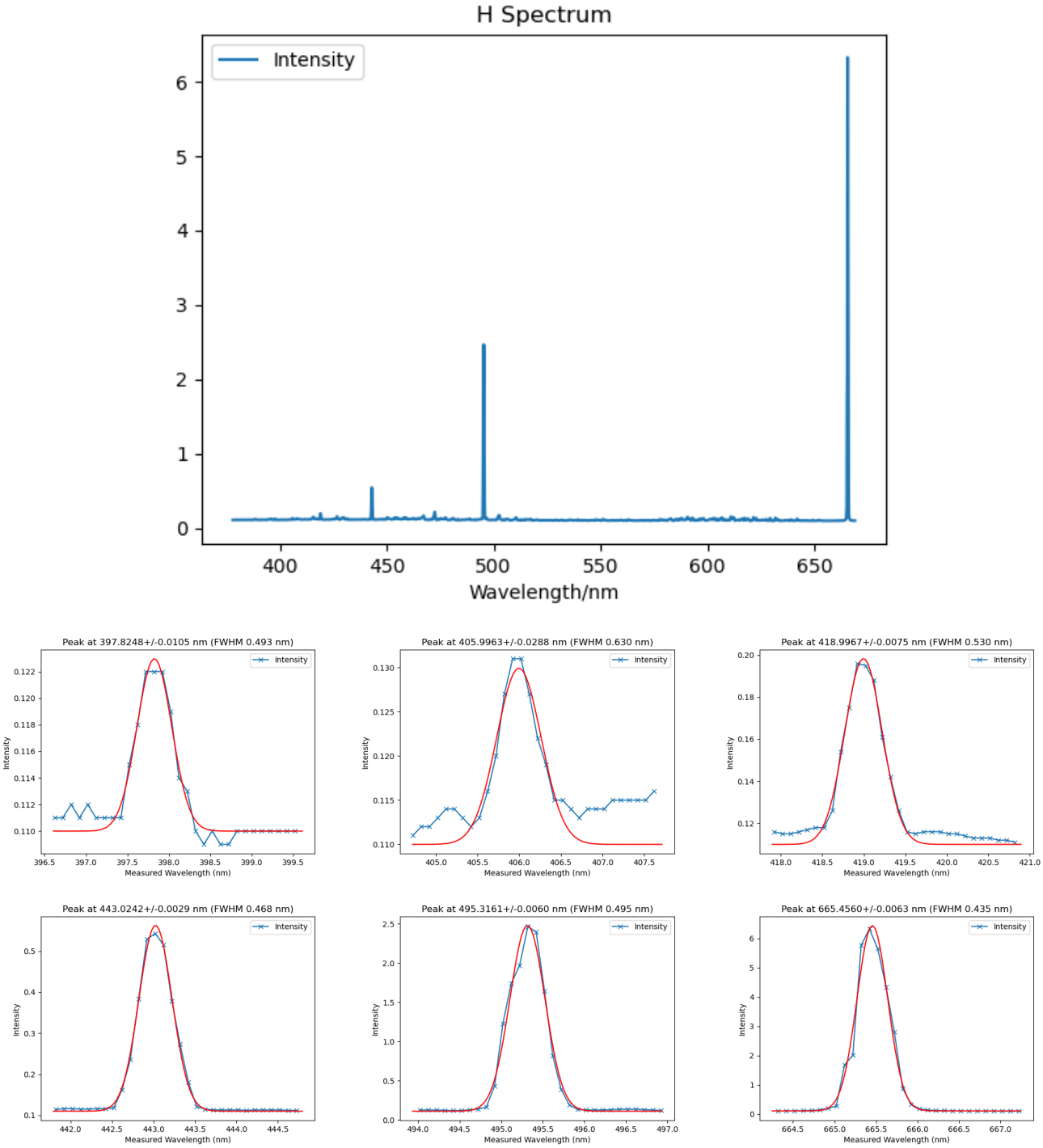

Figure 9. H Calibration Data

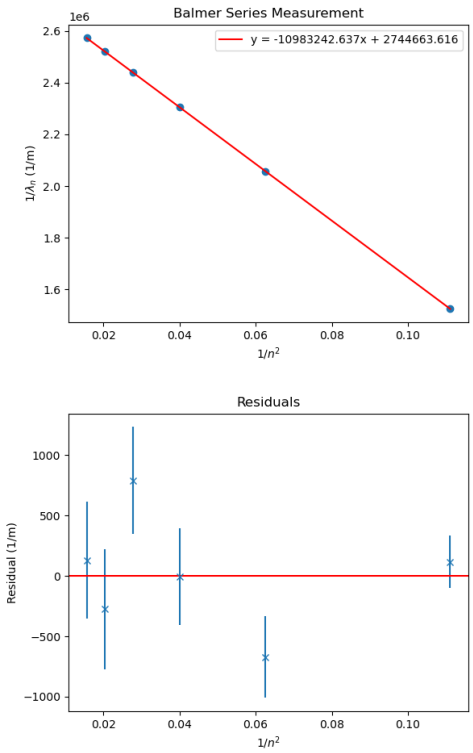

Figure 10. Balmer Series

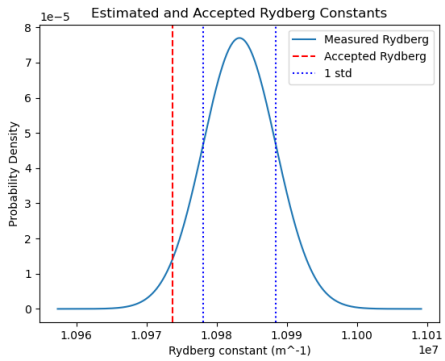

Figure 11. Rydberg Constant

strength we measure is always lower than that the Helium atoms experience. This systematic error could be mitigated in the future by using better measuring instruments and holding mechanisms, but since we are using a hand-held magnetometer to measure this field, we expect the magnetic field strength to be actually stronger. A stronger magnetic field strength would lead to a lower μ_B according to equation 7.

In conclusion, we measured the Bohr magneton and the Rydberg constant. The Rydberg constant mostly agrees with accepted values but the Bohr magneton does not. We identified potential ways to improve these measurements in future experiments but they will require more equipment.

6. ACKNOWLEDGEMENTS

Yubin Hu would like to thank his lab partner, Connor Jennings, for his help in performing this experiment.

REFERENCES

Holzapfel, W. 2023, ATM - Atomic Physics, http://experimentationlab.berkeley.edu/sites/default/files/writeups/ATM.pdf

Hunt, C. 2018, Zeeman Effect 012-14266A, https://advlabs.aapt.org/bfyiii/files/ZeemanEffect.pdf

Kramida, A., Yu. Ralchenko, Reader, J., & and NIST ASD Team. 2022, NIST Atomic Spectra Database (ver. 5.10), [Online]. Available: `https://physics.nist.gov/asd` [2023, April 10]. National Institute of Standards and Technology, Gaithersburg, MD.